

## Investigation of the $L_3$ - $M_{45}$ $M_{45}$ Auger spectra of Cu, $Cu_2O$ and CuO

This article has been downloaded from IOPscience. Please scroll down to see the full text article.

1992 J. Phys.: Condens. Matter 4 7607

(<http://iopscience.iop.org/0953-8984/4/37/008>)

View [the table of contents for this issue](#), or go to the [journal homepage](#) for more

Download details:

IP Address: 171.66.16.96

The article was downloaded on 11/05/2010 at 00:33

Please note that [terms and conditions apply](#).

## Investigation of the $L_3-M_{45}M_{45}$ Auger spectra of Cu, $Cu_2O$ and CuO

S R Barman and D D Sarma

Solid State and Structural Chemistry Unit, Indian Institute of Science, Bangalore 560 012, India

Received 13 January 1992, in final form 9 June 1992

**Abstract.** We report a comparative study of the  $L_3-M_{45}M_{45}$  Auger spectra of Cu,  $Cu_2O$  and CuO. The large intensity of the uncorrelated two-hole band-like spectrum in the  $L_3-M_{45}M_{45}$  Auger spectra of  $Cu_2O$  and CuO and the spectral shapes for these transitions indicate strong Cu 3d-O 2p hybridization in the oxides. The  $L_2-L_3M_{45}$  CK rates obtained for these compounds indicate the stability of the Cu 3d level with increasing oxidation state of Cu. We also provide a quantitative estimate of the contributions of the different processes that lead to the formation of the  $L_3-M_{45}M_{45}$  Auger satellite in Cu,  $Cu_2O$  and CuO.

### 1. Introduction

The  $L_{23}-M_{45}M_{45}$  Auger spectra of Cu which show the most intense and distinctly recognizable features in the Auger spectra of solids have been the subject of many investigations [1-13]. It has been suggested that the satellite accompanying the Cu  $L_3-M_{45}M_{45}$  spectrum is due to an  $L_3M_{45}-M_{45}M_{45}M_{45}$  Auger transition following an  $L_2-L_3M_{45}$  Coster-Kronig (CK) transition of an  $L_2$  hole [1]. This process effectively transfers spectral weight from the  $L_2-M_{45}M_{45}$  Auger spectrum of Cu to the satellite region (containing an extra  $M_{45}$  hole both in the initial and final states) of the  $L_3-M_{45}M_{45}$  Auger transition. The  $L_3M_{45}$  initial state, responsible for the satellite features, may also be generated following a CK decay of an  $L_1$  hole, namely the  $L_1-L_3M_{45}$  transition. Recently [10-13] it has been recognized that the satellite in the  $L_3-M_{45}M_{45}$  region may also be contributed by the direct generation of an  $L_3M_{45}$  state in the  $L_3$  photoemission process due to shake-up and shake-off transitions. The quantitative estimates for the different processes such as photoemission shake-up and shake-off and the CK decay of the  $L_2$  and  $L_1$  photo-holes contributing intensity to the  $L_3-M_{45}M_{45}$  Auger satellite of Cu have been worked out [13]. The oxides of Cu, namely  $Cu_2O$  and CuO, which have interesting electronic structures [14-17], also show intense Auger satellites accompanying the  $L_3-M_{45}M_{45}$  spectra. While the Cu 2p photoemission satellite due to shake-up in  $Cu_2O$  is very weak and similar to that in Cu, the 2p spectrum of CuO exhibit intense satellites. Therefore one expects a much larger satellite intensity for the  $L_3-M_{45}M_{45}$  spectrum of CuO compared with  $Cu_2O$  or Cu, but actually the satellite intensities in these three compounds are comparable. We decided to investigate the contributions of the different decay channels to the Auger satellite of  $L_3-M_{45}M_{45}$  spectra in  $Cu_2O$  and CuO. We have found that the

results for Cu and Cu<sub>2</sub>O are similar, but that in the Auger spectrum of CuO the L<sub>3</sub> photoemission shake-up channel makes a considerably larger contribution. We also show that the higher kinetic energy uncorrelated band part of the L<sub>3</sub>-M<sub>45</sub>M<sub>45</sub> Auger spectra in Cu<sub>2</sub>O and CuO exhibit pronounced effects of hybridization between the Cu 3d and O 2p states. We further calculate the transition probabilities of the L<sub>2</sub>-L<sub>3</sub>M<sub>45</sub> CK processes in Cu, Cu<sub>2</sub>O and CuO exhibiting the influence of the Cu 3d level energetics on the CK rates.

## 2. Experiment

The photoemission and the Auger spectra were recorded in the combined XPS-UPS-BIS instrument from VSW Scientific Instruments Ltd, UK. Measurements were carried out with laboratory sources (Al K $\alpha$  and Mg K $\alpha$ ). The spectrometer resolution for the Auger spectra was 0.2 eV, whereas the 2p core-level photoemission spectra were recorded with a total resolution of about 0.5 eV for monochromatic Al K $\alpha$  source and 0.9 eV for non-monochromatic Mg K $\alpha$  source. Commercially available CuO powder was sintered in flowing oxygen in the form of pellets. The sample surface was scraped with an alumina file in order to obtain a clean reproducible surface. Cu<sub>2</sub>O was prepared by precipitation following the reduction of concentrated copper acetate solution by 20% hydrazine hydrate solution [18]. Cu<sub>2</sub>O was studied in powdered form. The possible reduction of copper acetate to metallic copper on addition of excess hydrazine could be eliminated because of the absence of any signal due to Cu metal in the L<sub>23</sub>-M<sub>45</sub>M<sub>45</sub> Auger spectra of Cu<sub>2</sub>O. Also the possibility of contamination due to partial oxidation to CuO could be eliminated by noting the absence of the characteristic CuO 2p photoemission satellite signal. Metallic Cu was cleaned by argon-ion sputtering. The Auger spectra obtained with non-monochromatic Al K $\alpha$  and Mg K $\alpha$  and monochromatic Al K $\alpha$  sources showed no dependence on the excitation source.

## 3. Results and discussion

We show the L<sub>23</sub>-M<sub>45</sub>M<sub>45</sub> Auger spectra of Cu, Cu<sub>2</sub>O and CuO in figure 1. The most intense peak in each spectrum is due to the <sup>1</sup>G multiplet of the two-localized-hole d<sup>8</sup> final state [3]. The Auger spectra from the three samples have been aligned at the main peak for the purpose of comparison. The Auger satellite spectrum is distinct in each case, at about 4–8 eV kinetic energy below the <sup>1</sup>G peak. The sharp feature at about 921 eV kinetic energy in the spectrum for Cu is due to the <sup>3</sup>F multiplet of the localized d<sup>8</sup> final state [3]. This feature is not distinct in the spectra of Cu<sub>2</sub>O and CuO, due to strong broadening of the spectra in the oxides. However, our data analysis in terms of spectral fitting (see the appendix) clearly indicates the presence of these multiplets at about the same relative energy with respect to the <sup>1</sup>G peak. The broad feature above 922 eV kinetic energy is the signature of the delocalized two-hole final state in terms of the Cini-Sawatzky model [19, 20]. Comparing the L<sub>3</sub>-M<sub>45</sub>M<sub>45</sub> Auger spectra of Cu, Cu<sub>2</sub>O and CuO in the energy range between 922 eV and 930 eV kinetic energy clearly shows that the signatures of the delocalized two-hole state in the Auger spectra are more intense in Cu<sub>2</sub>O and CuO than in Cu. This part of the Auger spectrum is hardly discernible in the case of Cu (see

figure 1). The relative intensity of this part of the Auger spectrum compared with the transition arising from the localized two-hole final state is a function of  $U/W$  [20], where  $U$  is the effective intra-atomic Coulomb correlation strength and  $W$  is the relevant bandwidth; the delocalized signature in the Auger spectrum is expected to gain intensity with decreasing  $U/W$ . Thus the enhanced intensity in the spectral feature due to the delocalized two-hole final state is an indication of the decrease of effective  $U/W$  in Cu<sub>2</sub>O and CuO compared with Cu. It should be noted here, however, that the Cini-Sawatzky model which has provided the basis for the above interpretation, is itself based on a single-band model and is evidently of qualified use in the context of Cu<sub>2</sub>O and CuO. However, if we interpret  $W$  as the effective Cu 3d-O 2p hybrid bandwidth and note that the intra-atomic effective  $U$  in these systems do not change significantly (see text later), it appears that the effective  $W$  is larger for Cu<sub>2</sub>O and CuO than for Cu. This must be caused by the sizeable Cu 3d-O 2p hybridization interaction in the oxides, since the direct Cu 3d-Cu 3d interaction is expected to be very small in the oxides. It should also be noticed that the main peaks in the Auger spectra arising from the two-localized-correlated-hole final state are broader for Cu<sub>2</sub>O and CuO compared with Cu. There are several possible origins of this width. The Cu 2p photoemission spectra in Cu<sub>2</sub>O and CuO are considerably broader than that of Cu, contributing width to the Auger spectra. Of the two oxides, the Cu 2p photoemission spectrum of CuO has larger width. This may arise from the fact that the main peak of Cu<sub>2</sub>O 2p spectrum corresponds to a 2p-hole 3d<sup>10</sup> final state, while that of CuO is due to a 2p-hole 3d<sup>10</sup> configuration *with another hole in the ligand O 2p levels*. This ligand hole spans the whole O 2p bandwidth leading to an increased width of the spectral feature. The same effect then also contributes to the increased Auger spectral width in CuO. Moreover we note that the Cini-Sawatzky model provides another contribution to the Auger spectral widths for Cu<sub>2</sub>O and CuO. It has been shown that the width of the atomic-like correlated two-hole final state varies as  $W^2/U$ . Noting that  $W/U$  is larger in Cu<sub>2</sub>O and CuO compared with Cu, due to an increase in the effective bandwidth  $W$ , it is obvious that  $W^2/U$  will be larger for Cu<sub>2</sub>O and CuO than for Cu.

It is interesting to note that while the band-like uncorrelated two-hole final state feature is nearly absent in the spectrum of Cu and exhibits a broad pronounced feature in CuO, it exhibits a distinct two-peak structure in the case of Cu<sub>2</sub>O (marked by arrows in figure 1). Since the band-like spectrum is essentially governed by the self-convolution of the relevant part of the density of states, modified by the matrix element effects, we have compared this part of the Auger spectra of Cu<sub>2</sub>O and CuO to the self-convolution of the photoemission valence-band spectra of these compounds using 21.2 eV photon energy in a manner similar to that in [14]. The delocalized two-hole Auger spectra of CuO corresponds well in spectral shape and energy position to the self-convoluted density of states (DOS) obtained from valence-band photoemission [14]. We can estimate the effective screened intra-atomic Coulomb interaction strength,  $U_{dd}$ , within the Cu 3d manifold from the energy difference between the centroid of the self-convoluted DOS and the Auger spectral feature arising from the localized atomic-like two-hole final state; thus  $U_{dd}$  corresponding to the <sup>1</sup>G multiplet in CuO turns out to be 8.7 eV. In the case of Cu<sub>2</sub>O, the self-convoluted DOS shows [14] two distinct peaks at about 6.7 eV and 9.4 eV binding energy. The first peak at 6.7 eV arises from the presence of two uncorrelated 3d holes and the peak at 9.4 eV is due to an O 2p and a Cu 3d hole. The Auger spectrum in figure 1 clearly exhibits two features at about the same energies as in the self-convoluted DOS, indicating

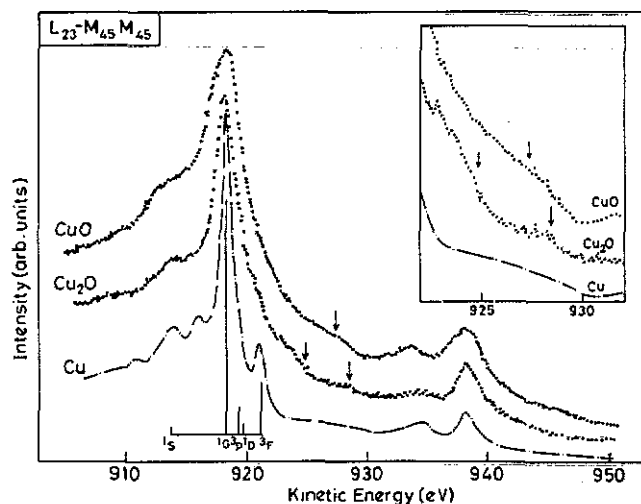


**Figure 1.** The  $L_{23}\text{-}M_{45}M_{45}$  Auger spectra of Cu (dot-dashed),  $\text{Cu}_2\text{O}$  and CuO (dots). The  $\text{Cu}_2\text{O}$  and CuO main peaks have been aligned to the main peak of Cu. The positions of the atomic-like features ( $^1G$ ,  $^3P$ ,  $^1D$  and  $^3F$ ) are indicated. The arrows indicate the two-hole band-like density of states features (also shown on an expanded scale in the inset) in  $\text{Cu}_2\text{O}$  and CuO.

that the  $L_3\text{-}M_{45}M_{45}$  Auger transition in the copper oxides not only generates two 3d holes, but also has a finite probability of generating an O 2p and a Cu 3d hole. This is only possible if there is a substantial overlap between the Cu 3d and O 2p states. The  $U_{dd}$  for  $\text{Cu}_2\text{O}$  is the energy difference between the feature due to the two uncorrelated 3d holes in the self-convoluted DOS and the localized atomic-like two-hole final state feature. Thus the estimate of  $U_{dd}$  corresponding to the  $^1G$  multiplet turns out to be 10.0 eV for  $\text{Cu}_2\text{O}$ . These estimates of  $U_{dd}$  are in agreement with previous ones [14].

**Table 1.** The relevant relative intensity ratios extracted from the Cu 2p photoemission spectra and the Cu  $L_{23}\text{-}M_{45}M_{45}$  Auger spectra of Cu,  $\text{Cu}_2\text{O}$  and CuO.

	Cu 2p photo-emission shake-up satellite/main peak ratio ( $\beta$ )	Cu $L_3\text{-}M_{45}M_{45}/L_2\text{-}M_{45}M_{45}$ main peak ratio ( $R$ )	Cu $L_3\text{-}M_{45}M_{45}$ satellite/main peak ratio
Cu	0.075	6.3	0.37
$\text{Cu}_2\text{O}$	0.05	5.7	0.36
CuO	0.45	4.2	0.47

We have extracted the intensities of the  $L_2\text{-}M_{45}M_{45}$  and  $L_3\text{-}M_{45}M_{45}$  transitions (without the satellite contributions) by spectral fitting as described in the appendix. The ratio ( $R$ ) of the  $L_3\text{-}M_{45}M_{45}$  and the  $L_2\text{-}M_{45}M_{45}$  spectral intensities decreases from Cu ( $R = 6.3$ ) to  $\text{Cu}_2\text{O}$  ( $R = 5.7$ ) and is substantially lower ( $R = 4.2$ ) in CuO (table 1). It is easy to see that the CK transition ( $L_2\text{-}L_3M_{45}$ ) probability transferring spectral weight from the  $L_2\text{-}M_{45}M_{45}$  region to the satellite of the  $L_3\text{-}M_{45}M_{45}$  region is given by  $(R - 2)/R$ , indicating that for  $R = 2$  the CK process is absent. This is

evident since  $R = 2$  implies that the intensity ratio between L<sub>3</sub>- and L<sub>2</sub>-M<sub>45</sub>M<sub>45</sub> is exactly according to the statistical branching ratio for the generation of the L<sub>3</sub> and L<sub>2</sub> initial-hole states and there is no transfer of intensity from the L<sub>2</sub>- to L<sub>3</sub>-M<sub>45</sub>M<sub>45</sub> transitions. The CK transition probabilities we get using the above expression are 0.68, 0.65 and 0.52 for Cu, Cu<sub>2</sub>O and CuO respectively. The L<sub>3</sub>-M<sub>45</sub>M<sub>45</sub> CK transition probability for Cu calculated by Yin *et al* [1] and McGuire [7], performed with neutral atom potential, is 0.64 and is in good agreement with the value obtained here. Note that earlier experimental estimates [21] of the intrinsic life-time widths of the L<sub>2</sub> and L<sub>3</sub> hole states suggest that the CK process probability for Cu L<sub>2</sub> holes is 0.62, in good agreement with the probability obtained here. Based on atomic calculations, it has been further pointed out [1, 7] that the rate of the CK process is very sensitive to the binding energy of the M<sub>45</sub> (3d) level, the rate of the L<sub>2</sub>-L<sub>3</sub>M<sub>45</sub> CK process decreasing with increasing binding energy. Thus the decreasing rate of the CK process in the series Cu, Cu<sub>2</sub>O and CuO can be related to the increasing stability of the Cu 3d level with increasing oxidation state of Cu.

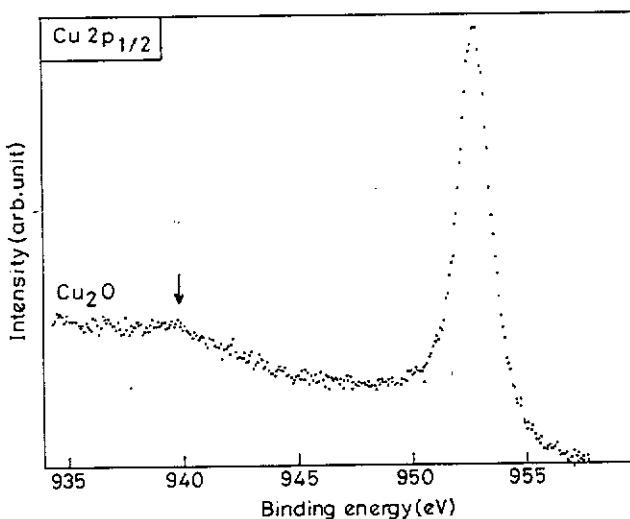


Figure 2. The Cu 2p<sub>1/2</sub> photoemission spectra of Cu<sub>2</sub>O, the arrow indicating the position of the weak satellite feature.

From our spectral fitting (see appendix), we have been able to obtain the intensity ratios between the satellite (three-hole and four-hole final states) and the main parts (two-hole final states) of the Auger spectra of Cu, Cu<sub>2</sub>O and CuO and these values are shown in table 1. We find that the satellite to main peak ratio for the L<sub>3</sub>-M<sub>45</sub>M<sub>45</sub> Auger spectra is higher in CuO than in Cu or Cu<sub>2</sub>O, the latter two compounds having comparable satellite intensity. In order to understand details of the origin of the Auger satellites in Cu<sub>2</sub>O and CuO, we have recorded the corresponding Cu 2p photoemission spectra. A weak 2p photoemission satellite is observed for Cu<sub>2</sub>O at about 12.7 eV higher binding energy from the main peak with a satellite to main peak intensity ratio of 0.05 (see figure 2 and table 1). This is comparable to the relative satellite intensity of 0.075 reported [13] for the 2p spectrum of Cu metal. For CuO, the 2p photoemission satellite to main peak intensity ratio (0.45) is much larger. The origin of these satellites has been discussed in detail in the literature; these represent primarily L<sub>23</sub>M<sub>45</sub> shake-up satellites.

For the following analysis it is important to note that the 3–4 eV decrease in the satellite to main peak energy separation in the Cu 2p photoemission spectrum of CuO compared to those in Cu<sub>2</sub>O and Cu has an important consequence. It is obvious that when  $U_{pd} + E_d + U_{dd}$  ( $U_{pd}$  is the Coulomb interaction strength between a Cu 2p hole and a 3d hole,  $E_d$  the energy of the Cu 3d hole and  $U_{dd}$  the Coulomb interaction strength between two 3d holes) is greater than the  $L_2$ – $L_3$  spin orbit splitting, the  $L_2M_{45}$  initial photo-hole will have a very low transition probability to decay via the  $L_2$ – $L_3M_{45}$  CK process. The energy separation between the photoemission satellite and the main peak in Cu provides an estimate of the strength of  $(U_{pd} + E_d)$ . Noting the satellite to main peak energy separation (about 12 eV) in the 2p photoemission spectrum and a  $U_{dd}$  of about 10 eV for Cu and Cu<sub>2</sub>O, it is evident that the initial  $L_2M_{45}$  photo-hole (the shake-up/shake-off satellites) cannot decay via the CK process in the case of Cu or Cu<sub>2</sub>O. But in CuO the 2p photoemission satellite is shifted 3–4 eV towards the main peak compared with Cu and Cu<sub>2</sub>O. Since  $U_{dd}$  in CuO remains comparable to  $U_{dd}$  in Cu and Cu<sub>2</sub>O, the decay of the  $L_2M_{45}$  shake-up satellite through the CK process becomes energetically allowed for CuO (unlike the cases of Cu and Cu<sub>2</sub>O). Thus one of the channels contributing intensity to the Auger satellite in the  $L_3$ – $M_{45}M_{45}$  region of CuO is the decay of the initial  $L_2M_{45}$  shake-up state via the  $L_2M_{45}$ – $L_3M_{45}M_{45}$  CK process to the  $L_3M_{45}M_{45}$  state which further undergoes an Auger decay to the  $(M_{45})^4$  four-hole final state. On the other hand, the shake-off channel  $L_2M_{45}O_p$  ( $O_p$  indicates a ligand hole) corresponding to the  $L_2$  photo-hole in CuO is energetically forbidden to undergo the CK transition. For the  $L_1$  photo-hole, the CK decay ( $L_1$ – $L_2M_{45}$  and  $L_1$ – $L_3M_{45}$ ) of both the shake-up and shake-off satellites are energetically allowed for all the three systems. We show in figure 3 all the decay processes of the  $L_3$ ,  $L_2$  and  $L_1$  photo-holes that are relevant for the  $L_3$ – $M_{45}M_{45}$  satellite intensity in these systems.

The different channels which contribute intensity to the  $L_3$ – $M_{45}M_{45}$  Auger satellite are the Auger decay of the  $L_3$  ( $2p_{3/2}$ ) photoemission shake-up/shake-off satellites and the CK decay of the photoemission main peak and the shake-up/shake-off satellites corresponding to  $L_2$  and  $L_1$  photo-holes (figure 3). The relative percentage contributions of these decay channels for Cu taken from [13] together with the satellite to main peak intensity ratio of 0.37 determined in the present study by spectral fitting indicate that the contributions of the above channels are 0.04, 0.07, 0.19 and 0.07 from shake-up, shake-off,  $L_2$  induced CK and  $L_1$  induced CK processes respectively. From these values for Cu, we can extrapolate the expected contributions of these channels to the satellite intensities in the  $L_3$ – $M_{45}M_{45}$  regions of Cu<sub>2</sub>O and CuO, using the experimental values of the 2p photoemission shake-up satellite to main peak intensity ratio ( $\beta$ ) and the  $L_3$ – $M_{45}M_{45}$ / $L_2$ – $M_{45}M_{45}$  main peak intensity ratio ( $R$ ) in this series and the details of the decay channels as shown in figure 3. Thus we find that the expected contribution of the  $L_2$  CK channel to the relative intensity of the satellite compared to the main peak in CuO is given by

$$0.19(1 + \beta_{CuO})[(R - 2)/R]_{CuO}/[(R - 2)/R]_{Cu}$$

where  $R = 2[1 + z/(x + y)]$  and the factor 0.19 is the  $L_2$  CK contribution to the relative satellite intensity in Cu. In the numerator, 1 and  $\beta_{CuO}$  (= 0.45) are the photoemission main peak/main peak and the shake-up satellite/main peak intensity ratios respectively for the  $L_2$  photo-hole of CuO. This way extrapolated contributions, the  $L_3$  photoemission shake-up channel, the  $L_3$  photoemission shake-off channel,

the CK decay of the  $L_2$  photo-hole and the CK decay of the  $L_1$  photo-hole to the relative intensity of the  $L_3$ - $M_{45}M_{45}$  Auger satellite are 0.03, 0.07, 0.18 and 0.07 respectively for  $Cu_2O$ . The corresponding numbers for CuO are 0.24, 0.09, 0.21 and 0.09 respectively. In this analysis it is assumed that the  $L_1$  photo-hole which has the CK channels  $L_1$ - $L_2M_{45}$  and  $L_1$ - $L_3M_{45}$ , decays through these CK channels with probability of  $k_2 = 0.18$  and  $k_3 = 0.39$  (which implies  $k_1 = 0.43$ , see figure 3) in accordance with the calculations of McGuire [7]. Since it is difficult to estimate the probability of the shake-off channel, in this analysis it is assumed to remain the same for  $Cu_2O$  and CuO as in Cu. The ratio of the photo-ionization cross sections [22] for the  $L_3$ ,  $L_2$  and  $L_1$  photo-holes is taken to be 2.0:1.0:0.55 in the calculation.

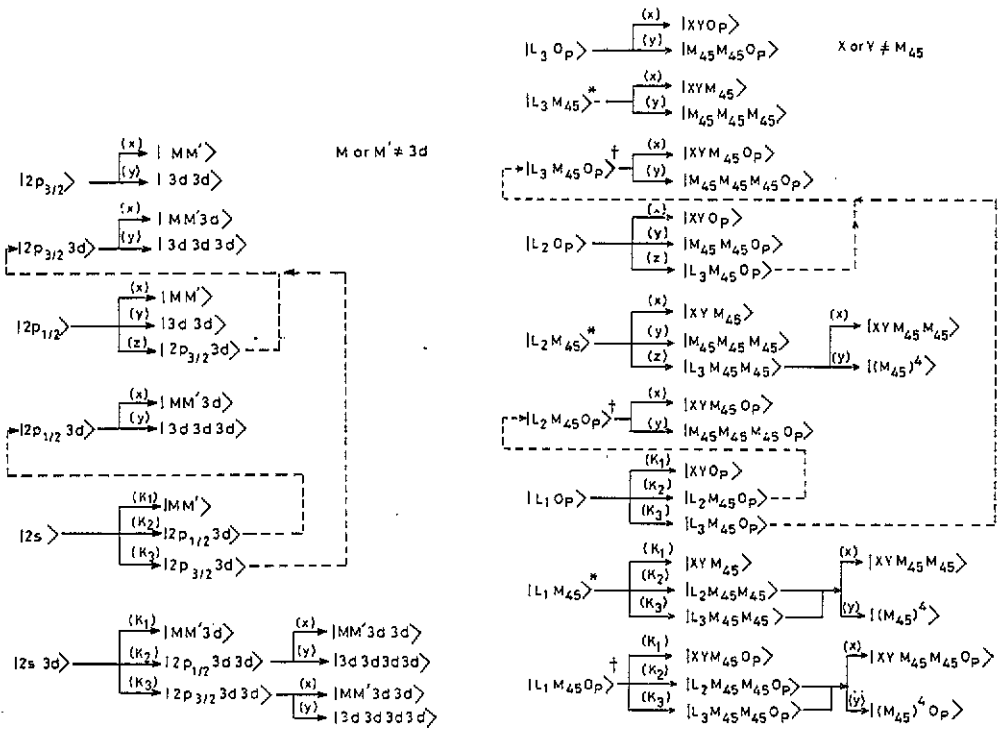


**Figure 3.** The decay processes for the  $L_3$ ,  $L_2$  and  $L_1$  holes in CuO which contribute to the  $L_3$ - $M_{45}M_{45}$  satellite intensity. The states are represented in a hole picture and the quantities in brackets indicate the probabilities of the corresponding decay processes. The bold arrows show the CK channels and the dashed arrows are used to connect the final state of a CK transition to the initial state of a subsequent Auger transition. The shake-up and the shake-off states are indicated by star (\*) and dagger (†) respectively. The symbol  $O_p$  indicates an  $O$  2p ligand hole state which is present both in the initial and final state of an Auger decay. The decay channels for Cu and  $Cu_2O$  are similar to that of CuO except for the CK decay of the  $L_2$  shake-up satellite which is energetically forbidden in these systems.

The contributions of the different decay channels in  $Cu_2O$  do not differ drastically from Cu. This is not surprising since the allowed decay channels for  $Cu_2O$  and Cu are the same (figure 3) and also the experimentally obtained inputs (i.e.  $\beta$  and  $R$ ) to the estimation of the various contributions are very similar between the two. In contrast CuO shows a marked difference compared with Cu (table 2). The contribution from



**Table 2.** The contribution of the different decay channels (the 2p photoemission shake-up, the 2p photoemission shake-off, the CK decay of the  $L_2$  photo-hole and the CK decay of the  $L_1$  photo-hole) to the  $L_3$ - $M_{45}M_{45}$  Auger satellite to main peak intensity ratio in Cu,  $Cu_2O$  and  $CuO$ . The numbers in the brackets are the relative percentage contributions.

	Photoemission shake-up	Photoemission shake-off	$L_2$ induced Coster-Kronig	$L_1$ induced Coster-Kronig
Cu	0.04 (11)	0.07 (18)	0.19 (52)	0.07 (19)
$Cu_2O$	0.03 (9)	0.07 (20)	0.18 (51)	0.07 (20)
$CuO$	0.24 (38)	0.09 (14)	0.21 (34)	0.09 (14)

the initial state shake-up channel increases by a factor of  $\beta_{CuO}/\beta_{Cu} \approx 6$  compared with Cu. The  $L_1$  CK contribution is also larger in  $CuO$  than in Cu. This is primarily because of the decrease of the  $L_3$  Auger main-peak intensity in  $CuO$  due to large  $\beta$ . This leads to the relative increase of the Auger satellite to main peak intensity ratio for the  $L_1$  CK channel contribution in  $CuO$ . Though the  $L_2$ - $L_3M_{45}$  CK decay rate in  $CuO$  is lower than that of Cu, large  $\beta$  and the CK decay of the  $L_2M_{45}$  shake-up satellite (which is forbidden in Cu) are the reasons for the larger contribution from the  $L_2$  CK process to the relative satellite intensity in the  $L_3$ - $M_{45}M_{45}$  Auger spectra.

The calculated relative intensity of the satellite for  $Cu_2O$  and  $CuO$ , which is the sum of the expected contributions from all four channels, should be in good agreement with the experimentally obtained relative satellite intensities. In the case of  $Cu_2O$ , the calculated value of 0.35 for the relative satellite intensity is in good agreement with the experimental value of 0.36 obtained from spectral fitting of the experimental Auger spectrum. For  $CuO$  the calculated relative satellite intensity is 0.63, whereas the experimental value is 0.47. This discrepancy is probably due to an overestimate of the shake-off probability in the  $CuO$  photoemission process, which was assumed to be equal to that in Cu. The overestimation of the shake-off probability results in increased contributions from the shake-off and the  $L_1$  CK channel to the relative satellite intensity in the  $L_3$ - $M_{45}M_{45}$  Auger spectra of  $CuO$ . Besides the overestimation of the shake-off probability accompanying the initial state core-hole creation in the case of  $CuO$ , errors can also arise from the experimental estimates of different satellite intensities. In this context it should be realized that these estimates can contain up to a 20% uncertainty. The estimate of the other channels contributing to the relative satellite intensities in the  $L_3$ - $M_{45}M_{45}$  Auger spectra of these compounds are quite reliable however, since the processes responsible (e.g. the shake-up and the CK rates) have been experimentally determined here.

In conclusion we have shown that the  $U_{dd}$  values for  $Cu_2O$  and  $CuO$  are comparable. The uncorrelated two-hole band-like spectrum of the  $L_3$ - $M_{45}M_{45}$  transition has large intensity for  $CuO$  and  $Cu_2O$  compared with that for Cu, indicating an increase of the effective bandwidth due to the hybridization of the Cu 3d states with the O 2p states. The spectral shapes for these transitions provide further evidence for the extensive Cu 3d-O 2p hybridization in the oxides. The  $L_2$ - $L_3M_{45}$  CK rates have been obtained for Cu,  $Cu_2O$  and  $CuO$  from the observed intensity ratio between the  $L_3$ - $M_{45}M_{45}$  and the  $L_2$ - $M_{45}M_{45}$  transitions, the trends in the CK rates indicating an increasing stability of the Cu 3d states in the series Cu,  $Cu_2O$  and  $CuO$ , in agreement with previous calculations. Using these CK rates and the experimentally obtained shake-up satellites intensities of the Cu spectra in these compounds, we

provide quantitative estimates for the contributions of the various decay channels to the Auger satellite intensity.

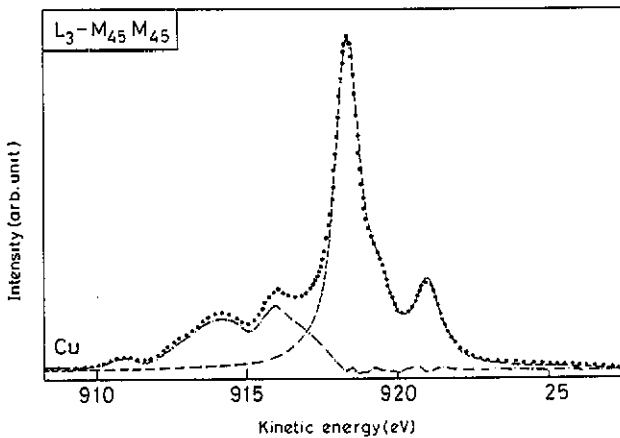


Figure 4. The  $L_3-M_{45}M_{45}$  Auger spectrum of Cu (dots), the main peak of the  $L_3-M_{45}M_{45}$  Auger spectrum obtained by least-square error fitting (dashed curve), and the satellite part of the  $L_3-M_{45}M_{45}$  Auger spectrum (dot-dashed curve) obtained by subtracting the previous two curves.

### Acknowledgments

We thank Professor C N R Rao for his continued support. We thankfully acknowledge the financial support of the Department of Science and Technology, Government of India. One of us (SRB) is thankful to the Council of Scientific and Industrial Research for a research fellowship.

### Appendix

We have analysed the spectral features by fitting the experimentally obtained  $L_3-M_{45}M_{45}$  Auger spectra in terms of a least-square error approach. First, the spectra were background subtracted using an iteration procedure. In each case, the most intense peak was associated with the  $^1G$  multiplet of the final  $d^8$  configuration. All the multiplets  $^1G$ ,  $^3P$ ,  $^1D$  and  $^3F$  which appear in the Auger main peak (excepting  $^1S$  which is neglected assuming its intensity to be insignificant) were represented by a Gaussian of fixed width of 0.2 eV representing the spectrometer resolution function. These Gaussian broadened multiplets were then convoluted with a Lorentzian whose width was varied as a parameter in the fitting routine. Besides the main peak due to the  $^1G$  state in all cases, the  $^3F$  feature is also sharply defined for Cu. The position of the other two multiplets ( $^3P$  and  $^1D$ ) for Cu was determined using the least-square error routine by scanning the energy region between  $^1G$  and  $^3F$ . If we take the position of the  $^1G$  as reference, the positions of  $^3P$ ,  $^1D$  and  $^3F$  on the basis of the above analysis turn out to be +1.0, +1.3 and +2.7 eV respectively. These values agree fairly well with the earlier theoretical calculations which give the relative separation

of the  $^3P$ ,  $^1D$  and  $^3F$  multiplets with respect to  $^1G$  to be +0.6, +1.0 and +3.0 eV [2] and +0.7, +1.2 and +3.3 eV [3]. One important point to be noted here is that the least-square error fitting was done taking only the part of the experimental spectra on the higher kinetic energy side of the  $^1G$  peak which has no satellite contribution. This is done to ensure that the fitted  $L_3-M_{45}M_{45}$  Auger main peak spectral shape has no satellite contribution. A Gaussian was used to represent the uncorrelated two-hole band-like part of the Auger spectra. A scaling factor was also introduced in the fitting routine in order to vary the multiplet positions with respect to the  $^1G$  multiplet by a multiplicative constant. The satellite was extracted by subtracting the least-square error fitted  $L_3-M_{45}M_{45}$  main peak from the experimental  $L_3-M_{45}M_{45}$  spectra containing both the satellite and the main peak contribution (figure 4). The same procedure was applied for  $Cu_2O$  and  $CuO$ . The relative multiplet positions in  $Cu_2O$  and  $CuO$  were found to be similar to that of  $Cu$ . We used two Gaussians in  $Cu_2O$  and one Gaussian in  $CuO$  to represent the uncorrelated two-hole band-like density of states.

## References

- [1] Yin L I, Adler I, Chen M H and Crasemann B 1973 *Phys. Rev. A* **7** 897
- [2] Kowalczyk S P, Pollack R A, McFeeley F R, Ley L and Shirley D A 1973 *Phys. Rev. B* **8** 2387
- [3] Yin L I, Adler I, Tsang T, Chen M H, Ringers D A and Crasemann B 1974 *Phys. Rev. A* **9** 1070
- [4] Roberts E D, Weightman P and Johnson C E 1975 *J. Phys. C: Solid State Phys.* **8** L301
- [5] Antonides E and Sawatzky G A 1976 *J. Phys. C: Solid State Phys.* **9** L547
- [6] Haak H W, Sawatzky G A and Thomas T D 1978 *Phys. Rev. Lett.* **41** 1825
- [7] McGuire E J 1971 *Phys. Rev. A* **3** 1801; 1978 *Phys. Rev. A* **17** 182
- [8] Weightman P and Andrews P T 1979 *J. Phys. C: Solid State Phys.* **12** 943
- [9] Mårtensson N and Johansson B 1983 *Phys. Rev. B* **28** 3733
- [10] Sarma D D, Carbone C, Sen P, Cimino R and Gudat W 1989 *Phys. Rev. Lett.* **63** 656
- [11] Wassdahl N, Rubensson J-E, Bray G, Glans P, Bleckert P, Nyholm R, Cramm S, Mårtensson S and Nordgren J 1990 *Phys. Rev. Lett.* **64** 2807
- [12] Sarma D D, Carbone C, Sen P, Cimino R and Gudat W 1991 *Phys. Rev. Lett.* **66** 967
- [13] Sarma D D, Barman S R, Cimino R, Carbone C, Sen P, Roy A, Chainani A and Gudat W 1992 *Phys. Rev. B* submitted
- [14] Ghijsen J, Tjeng L H, van Eip J, Eskes H, Westerink J, Sawatzky G A and Czyzyk M T 1988 *Phys. Rev. B* **38** 11322
- [15] Ghijsen J, Tjeng L H, Eskes H, Sawatzky G A and Johnson R L 1990 *Phys. Rev. B* **42** 2268
- [16] Shen Z-X, List R S, Dessau D S, Parmigiani F, Arko A J, Bartlett R, Wells B O, Lindau I and Spicer W E 1990 *Phys. Rev. B* **42** 8081
- [17] Tjeng L H, Chen C T, Ghijsen J, Rudolf P and Sette F 1991 *Phys. Rev. Lett.* **67** 501
- [18] Brauer G 1967 *Handbook of Preparative Inorganic Chemistry* vol 2, 2nd edn (London: Academic) p 1011
- [19] Cini M 1976 *Solid State Commun.* **20** 605; 1977 *Solid State Commun.* **24** 681
- [20] Sawatzky G A 1977 *Phys. Rev. Lett.* **39** 504
- [21] Nyholm R, Mårtensson N, Lebugle A and Axelsson U 1981 *J. Phys. F: Met. Phys.* **11** 1727
- [22] Yeh J J and Lindau I 1985 *At. Data Nucl. Data Tables* **32** 1